

## Carbon Isotope Fractionation During Volatilization of Petroleum Hydrocarbons and Diffusion Across a Porous Medium: A Column Experiment

DANIEL BOUCHARD,<sup>†</sup> PATRICK H ÖHENER,<sup>‡</sup> AND DANIEL HUNKELER\*<sup>·†</sup>

Center for Hydrogeology, University of Neuchâtel, Rue Emile Argand 11, CH-2009 Neuchâtel, Switzerland

Laboratoire Chimie Provence, UMR 6264, Universités d'Aix-Marseille I, II et III-CNRS, Case 29, 3, Place Victor Hugo, F-13331 Marseille Cedex 3, France

The study focuses on the effect of volatilization, diffusion, and biodegradation on the isotope evolution of volatile organic compounds (VOCs) in a 1.06 m long column filled with alluvial sand. A liquid mixture of 10 VOCs was placed at one end of the column, and measurements of VOC vapor concentrations and compound-specific isotope ratios ( $\delta^{13}\text{C}$ ) were performed at the source and along the column. Initially, the compounds became depleted in  $^{13}\text{C}$  by up to  $-4.8\text{‰}$  along the column axis, until at 26 h, uniform isotope profiles were observed for most compounds, which is expected for steady-state diffusion. Subsequently, several compounds (*n*-pentane, benzene, *n*-hexane) became enriched in  $^{13}\text{C}$  throughout the column. For the same compounds, a significant decrease in the source vapor concentration and a gradual enrichment of  $^{13}\text{C}$  by up to  $5.3\text{‰}$  at the source over a period of 336 h was observed. This trend can be explained by a larger diffusive mass flux for molecules with light isotopes compared to those with a heavy isotope, which leads to a depletion of light isotopes in the source. The isotope evolution of the source followed closely a Rayleigh trend and the obtained isotope enrichment factor corresponded well to the ratio between the diffusion coefficients for heavy and light molecules as expected based on theory. In contrast to diffusion, biodegradation had generally only a small effect on the isotope profiles, which is expected because in a diffusion-controlled system the isotope shift per decrease of mass flux is smaller than in an advection-controlled system. These findings open interesting perspectives for monitoring source depletion with isotope and have implications for assessing biodegradation and source variability in the unsaturated zone based on isotopes.

### Introduction

Widespread use of petroleum hydrocarbons as primary source of energy unfortunately leads to frequent spills of these nonaqueous phase liquids (NAPLs) into soils. Spilled NAPLs migrate downward through the unsaturated zone in response to gravity-driven force and result in subsurface contamination. Frequently, a fraction of the spilled NAPL is retained in the pores of the unsaturated zone (1) and creates a contaminant source from which volatile organic compounds (VOCs) are emanating for potentially long periods. In the unsaturated zone, diffusion is frequently an important transport process for VOCs (2) although density-driven advection can play a role, too (3). VOCs can undergo biodegradation in the soil–water phase restricting the transfer of contaminants to groundwater or atmosphere.

Numerous studies have made use of compound-specific isotope analysis in the saturated zone to demonstrate in situ

biodegradation of petroleum hydrocarbon and chlorinated solvents (4) and to distinguish between different sources of these compounds (5). The same approach can potentially also been used in unsaturated zone studies. However, much less is known about the isotope evolution during volatilization, diffusion, and biodegradation of organic compounds under unsaturated conditions. Most studies on volatilization focused on isotope effects during volatilization of a pure organic liquid. It was shown already more than 50 years ago that hydrophobic compounds with a  $^{13}\text{C}$  have slightly higher vapor pressures than their counterparts with  $^{12}\text{C}$  (6, 7). This isotope effect was explained by lower molar volumes and intermolecular attraction of compounds with heavy isotopes, which are thus more volatile (8). Later studies confirmed a small enrichment of  $^{13}\text{C}$  in the headspace above a liquid phase in closed vessels for petroleum hydrocarbons (9–11), and a larger effect for chlorinated solvents (9, 12, 13). A similar effect was also observed during kinetic evaporation from open vessels (11, 12, 14). Based on the results of all these experiments, it was concluded that the remaining liquid NAPL and hence the vapor phase should get depleted in  $^{13}\text{C}$  with time.

Several studies demonstrated the occurrence of isotope fractionation during diffusion of methane, ethane, propane, and butane through different media (15–18). In laboratory and field studies (19) carbon isotope fractionation during transport of  $\text{CO}_2$  in the gas phase of the unsaturated zone was also observed. Due to the presence of a heavy isotope in the molecule,  $^{13}\text{CO}_2$  was found to diffuse more slowly than  $^{12}\text{CO}_2$  which caused isotope fractionation with distance. In a recent field experiment (20), it was demonstrated that a diffusion isotope effect also occurs for VOCs. An initial depletion of  $^{13}\text{C}$  in VOCs with increasing distance from the source was observed followed by an enrichment of  $^{13}\text{C}$ . In the same study, it became evident that the source also underwent isotopic changes, calling for a further analysis of isotope fractionation associated with source aging by volatilization and degradation.

The main aim of this study was to gain more detailed insight into carbon isotope fractionation during volatilization of petroleum hydrocarbons and diffusion across a porous medium, and to derive a quantitative relationship to describe the isotope evolution of the source. For this purpose, a column experiment was carried out which allowed the study of isotope fractionation in great detail under controlled conditions. Based on a previous experiment with the same column (21) it was expected that some compounds will degrade in the column at different rates, which makes it possible to evaluate the effect of biodegradation on the observed isotope profiles as well.

\* Corresponding author phone: +41 32 718 2560; fax + 41 32 718 26 03; e-mail: daniel.hunkeler@unine.ch.

<sup>†</sup> University of Neuchâtel.

<sup>‡</sup> Universités d'Aix-Marseille.

**TABLE 1. Composition of the Fuel Mixture with Expected Initial Concentration at the Source (According to Raoult's Law), Measured Concentration at the Source at  $t = 12$  h, Molecular Gas-Phase Diffusion Coefficients  $D_{m,i}$ , Ratio of Diffusion Coefficients for Light and Heavy Molecules According to Eq 4 and Biodegradation Rate Constants  $k_i$**

compound	weight in mixture (%)	expected air phase conc. (g/m <sup>3</sup> )	measured air phase conc. at $t = 12$ h (g/m <sup>3</sup> )	$D_{m,i}^a$ (m <sup>2</sup> /d)	$(^hD_{m,i}/D_{m,i} - 1) \cdot 1000$ (‰)	$k_i$ this study (d <sup>-1</sup> )	$k_i^b$ previous study (d <sup>-1</sup> )
<i>n</i> -pentane	4.6	129.2	107.1	0.7211	-2.18		<0.01
<i>n</i> -hexane	9.6	77.5	70.9	0.6268	-1.62	0.34	0.26
<i>n</i> -octane	10.3	7.9	6.8	0.5275	-0.99	3.25	5.0
<i>n</i> -decane	18.6	1.8	0.9	0.4630	-0.62		13.5
benzene	2.6	13.5	10.8	0.7981	-1.91	0.36	
toluene	4.1	6.1	4.3	0.7271	-1.44		1.31
<i>m</i> -xylene	5.7	2.5	1.6	0.5892	-1.13		3.28
isooctane (2,2,4-trimethyl-pentane)	17.7	42.1	32.7	0.5275	-0.99	0.09	0.09
methyl-cyclohexane	12.6	30.0	22.8	0.5863	-1.29	0.11	0.16
1,2,4-trimethyl-benzene	14.4	1.7	0.7	0.6080	-0.91		4.98

<sup>a</sup> From ref 27. <sup>b</sup> From ref 21.

## Materials and Methods

**Column Experiment.** A liquid mixture of 10 volatile organic compounds commonly found in gasoline was prepared (Table 1). The percentages of the less volatile compounds were higher than in typical gasoline in order to increase the lifetime of the source. All organic compounds were obtained from Fluka (Buchs, Switzerland) in their purest form.

The selected alluvial sand was previously used to evaluate the biodegradation of volatile gasoline compounds, and the physicochemical characteristics of the sand were thus known (21). The sand was sieved at 4 mm and no microbial cultures were added to the indigenous population. The total porosity of the sand packed in the column was estimated as 0.41, the organic carbon content ( $f_{oc}$ ) was 0.2% and the water content, calculated by gravimetric mass loss after drying at 105 °C, was 3.3%.

The experimental setup and the dimensions of the cylindrical column are illustrated in Supporting Information (SI) Figure S1. The column consisted of a steel cylinder with a length of 1.20 m and an internal diameter of 8.1 cm that can be tightly closed at both ends with steel caps and Teflon O-rings. The column was filled with moist sand which was firmly compacted. At both ends, void chambers of 7 cm depth were created by removing moist sand. The clean-cut edges of the compacted moist sand remained stable without any need of support. An open vessel containing 10 mL of the hydrocarbon mixture (Table 1) was emplaced at one end of the column and the chamber was then immediately closed with the steel caps. The exit chamber at the opposite end of the column was constantly purged with humidified air at a rate of about 5 mL/minute to evacuate VOCs out of the chamber into a bag with activated charcoal. Vapor samples were collected using gastight syringes (Hamilton Company, Geneva, Switzerland) and steel needles (26 s/2"/2 L) pierced through samplings ports which consisted of 4.8 mm holes closed with GC septa (injection rubber plugs, Shimadzu, Kyoto, Japan). The room temperature was recorded every 30 min and remained stable at  $23.5 \pm 0.5$  °C during the whole experiment.

**Analytical Methods.** Vapor samples were analyzed using a TRACE gas chromatograph (GC) coupled to an ThermoFinnigan Delta Plus XP isotope-ratio mass spectrometer via a ThermoFinnigan GC combustion III interface. Injections were performed using a loop injector and varied from 50 to 1000  $\mu$ L to ensure a minimum delivery of 1 nmol of carbon to the GC column. A nitrogen-cryogenic system was used for the 250 and 1000  $\mu$ L loops to focus the analytes into a narrow band. The carrier gas was helium with a flow rate of 1.7 mL

min<sup>-1</sup> and the oxidation reactor was set to 940 °C. A BGB-5 column (BGB Analytik, Böckten, Switzerland, 30 m  $\times$  0.25 mm i.d.) was used to separate the compounds. Concentrations were determined based on the combined peak area of all three CO<sub>2</sub> mass ions (44, 45, and 46) of samples using external standards. Standard deviations were  $\pm 5\%$  ( $n = 5$ ) for concentrations and 0.3‰ ( $n = 5$ ) for isotope analysis. Isotope ratios are reported using the  $\delta^{13}C$  notation (in ‰) relative to the VPDB standard (22) according to the following:

$$\delta^{13}C = \left( \frac{R_{\text{sample}}}{R_{\text{reference}}} - 1 \right) \cdot 1000 \quad (1)$$

where  $R_{\text{sample}}$  and  $R_{\text{reference}}$  are the ratio of <sup>13</sup>C/<sup>12</sup>C of the measured sample and the VPDB reference, respectively.

**Quantifying Isotope Fractionation at the Source Due to Volatilization and Diffusion.** As demonstrated in a detailed mathematical derivation in S1 of the Supporting Information, the isotope evolution of a compound *i* in a NAPL source subject to volatilization and diffusion across a porous medium is expected to follow a Rayleigh trend. The isotope fractionation factor is expected to correspond to the product of the ratio of vapor pressures,  $^hP_i/{}^lP_i$ , multiplied by the ratio of gas-phase diffusion coefficient,  $^hD_{m,i}/{}^lD_{m,i}$  (S1, Supporting Information):

$$\alpha_{\text{source},i} = \frac{{}^hD_{m,i}}{{}^lD_{m,i}} \cdot \frac{{}^hP_i}{{}^lP_i} \quad (2)$$

where  ${}^lP_i$  and  ${}^hP_i$  are the vapor pressures of molecules with light isotopes only and molecules with one heavy isotope, respectively;  ${}^lD_{m,i}$  and  ${}^hD_{m,i}$  the gas-phase diffusion coefficients of molecules with light isotopes only and molecules with one heavy isotope, respectively. The corresponding isotope enrichment factors can be calculated according to

$$\varepsilon_{\text{source},i} = (\alpha_{\text{source},i} - 1) \cdot 1000 \quad (3)$$

The theoretical ratio between the diffusion coefficients is given by (19, 23)

$$\frac{{}^hD_{m,i}}{{}^lD_{m,i}} = \sqrt{\frac{M_{wl,i}(M_{wh,i} + M_a)}{M_{wh,i}(M_{wl,i} + M_a)}} \quad (4)$$

where  $M_{wl,i}$  and  $M_{wh,i}$  are the molecular weights of molecules with light isotopes only and one heavy isotope, respectively, and  $M_a$  is the average molecular weight of soil air.

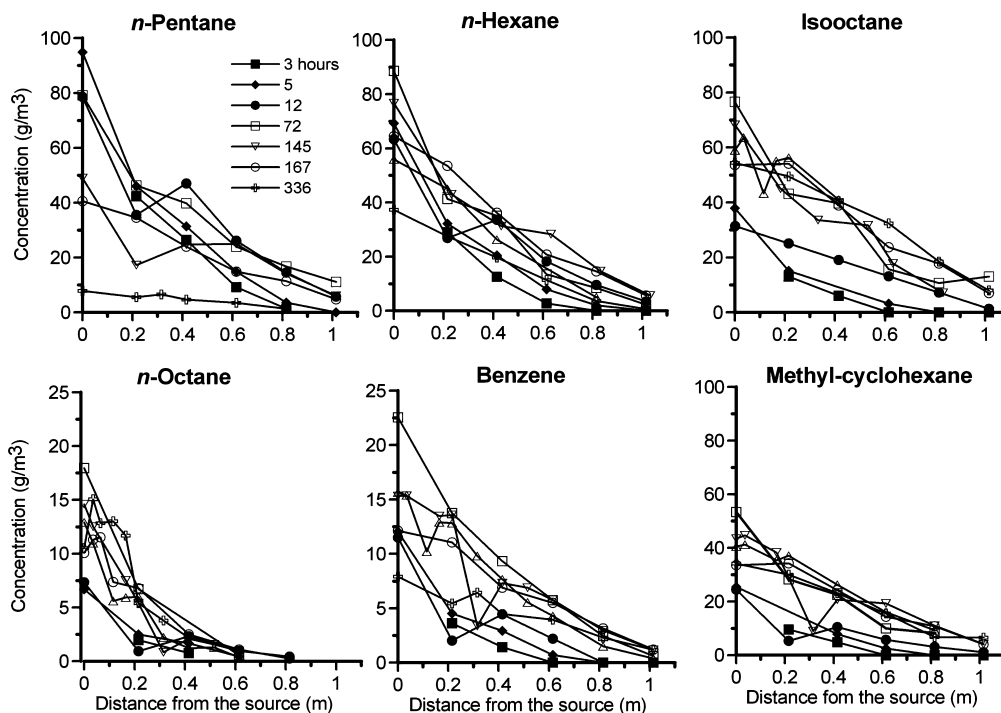


FIGURE 1. Concentration profiles evolution of VOCs in the column at selected times.

The experimental isotope enrichment factors can be determined using the Rayleigh equation (24):

$$1000 \cdot \ln \frac{R}{R_0} = 1000 \cdot \ln \frac{\delta^{13}\text{C}/1000 + 1}{\delta^{13}\text{C}_0/1000 + 1} = \varepsilon \cdot \ln \frac{C}{C_0} \quad (5)$$

where  $\delta^{13}\text{C}_0$  and  $\delta^{13}\text{C}$  are the initial isotope ratio of a compound and the isotope ratio at time  $t$ , respectively;  $C_0$  and  $C$  the initial concentration and the concentration at time  $t$ , respectively. The isotope enrichment factor can be quantified by plotting the second expression versus  $\ln C/C_0$  and carrying out a linear regression.

## Results

The temporal variations of VOC concentrations are illustrated in Figure 1 for compounds present at concentrations  $>5 \text{ g/m}^3$ . For the other compounds with lower concentrations, only limited data sets were obtained that are not presented. For the selected compounds, the measured concentration at the source after 12 h deviated by less than 25% from expected concentrations based on Raoult's law (Table 1) indicating that volatilization took place at or close to equilibrium conditions. Typical diffusion-controlled concentration profiles were observed with decreasing concentrations as a function of distance (Figure 1). *n*-Pentane and *n*-hexane were the first compounds to reach the end of the column (within 12 h). In contrast, *n*-octane was never detected further away than 0.8 m. The concentration profiles measured later than 72 h for methylcyclohexane (MCH), isooctane and *n*-octane remained fairly stable until the end of the experiment. The concentration profiles for *n*-pentane were observed to decrease with time after more than 72 h until almost complete depletion at 336 h, while for *n*-hexane and benzene, a decrease in concentration was noted after more than 145 h. Based on the concentration profiles at 96 or 145 h, first order biodegradation rate constants were estimated by fitting an analytical solution of the 1D diffusion-reaction equation to the data (for details see S2 in the Supporting Information). The degradation rates (Table 1) were in the same range as rates obtained during a previous study with the same column and same packing (21).

The  $\delta^{13}\text{C}$  varied in space and time and the extent of variation was compound dependent (Figure 2). Generally, lighter compounds (e.g., *n*-pentane) exhibited larger isotopic variations than heavier compounds (e.g., *n*-octane). Early after the source emplacement, the compounds became depleted in  $^{13}\text{C}$  with increasing distance with respect to the pure compound values. The maximal  $\delta^{13}\text{C}$  shift at  $t = 5 \text{ h}$  was as follows:  $-4.8\text{‰}$  for *n*-pentane,  $-3.8\text{‰}$  for *n*-hexane,  $-2.8\text{‰}$  for benzene,  $-2.1\text{‰}$  for *n*-octane,  $-1.7\text{‰}$  for MCH, and  $-1.4\text{‰}$  for isooctane. With time, the shifts became smaller until at time  $t = 26 \text{ h}$ , the isotope ratio of all compounds had generally leveled out with distance at the  $\delta^{13}\text{C}$  value of the pure compound. Afterward, a different  $\delta^{13}\text{C}$  evolution was observed for different compounds. The isotope ratios of MCH and isooctane remained unchanged close to the initial isotope ratio of the source chamber, except for a small increase in  $\delta^{13}\text{C}$  with distance for MCH after 336 h. *n*-Pentane and benzene also showed a uniform isotope ratio profile that, however, shifted upward after  $>26 \text{ h}$  for *n*-pentane and  $>168 \text{ h}$  for benzene. The  $\delta^{13}\text{C}$  of *n*-hexane at  $t = 72 \text{ h}$  and  $96 \text{ h}$  (Figure 2) tended to increase with increasing distance from the source, whereas at  $t = 168 \text{ h}$  the entire profile was in addition shifted upward by about  $1\text{‰}$ .

The vapor concentration and  $\delta^{13}\text{C}$  values monitored in the source chamber during 14 days are illustrated in Figure 3. Over the whole duration of the experiment, the concentration of *n*-pentane, *n*-hexane, and benzene decreased to between 0.06, 0.45, and 0.55, respectively, of their initial value, whereas the concentrations of MCH, *n*-octane and isooctane increased to 1.13, 1.23, and 1.20, respectively, times their initial value likely due to an increase of their mole fraction in the mixture. The  $\delta^{13}\text{C}$  of *n*-pentane, *n*-hexane, and benzene increased by more than  $1\text{‰}$ , whereas the  $\delta^{13}\text{C}$  of MCH, *n*-octane, and isooctane remained close to the  $\delta^{13}\text{C}$  of the corresponding pure compound apart from a small increase of the  $\delta^{13}\text{C}$  of *n*-octane after more than 268 h.

## Discussion

The concentration evolution of the VOCs followed similar patterns as reported and discussed in a previous study using

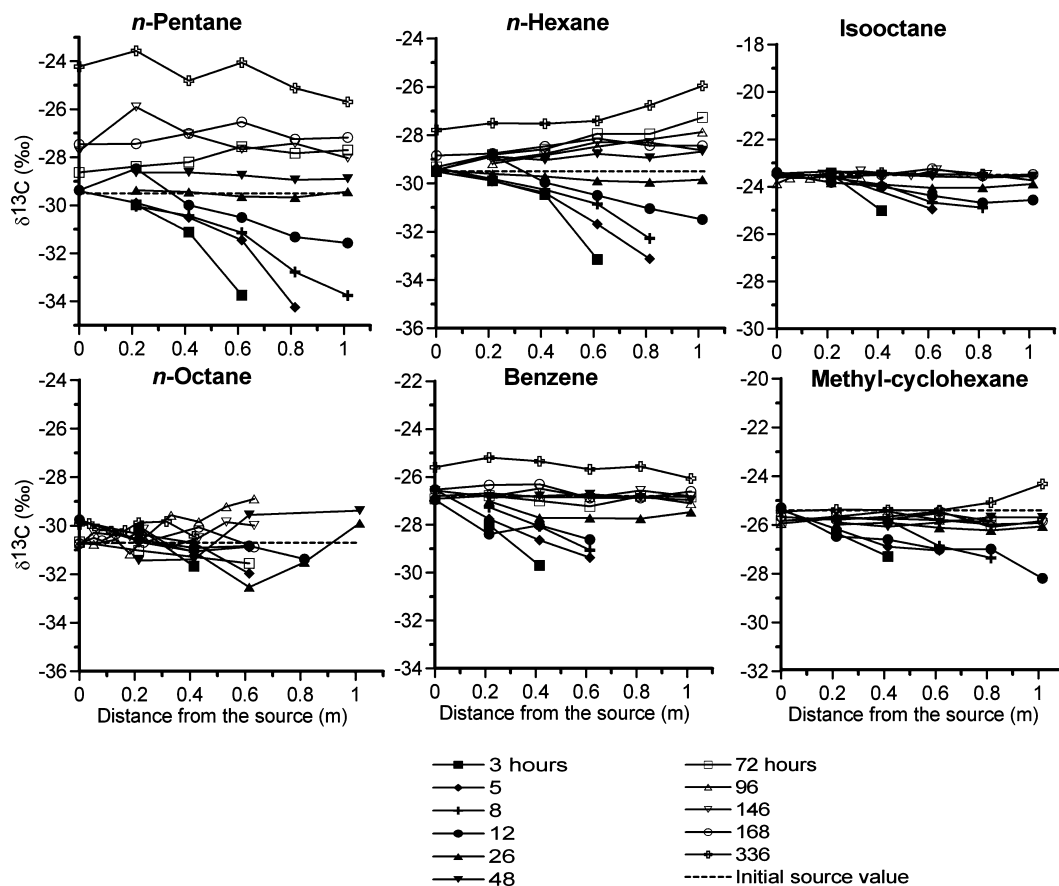


FIGURE 2.  $\delta^{13}\text{C}$  values in the column at selected times. The dashed lines illustrate the  $\delta^{13}\text{C}$  of the pure compounds used in the study.

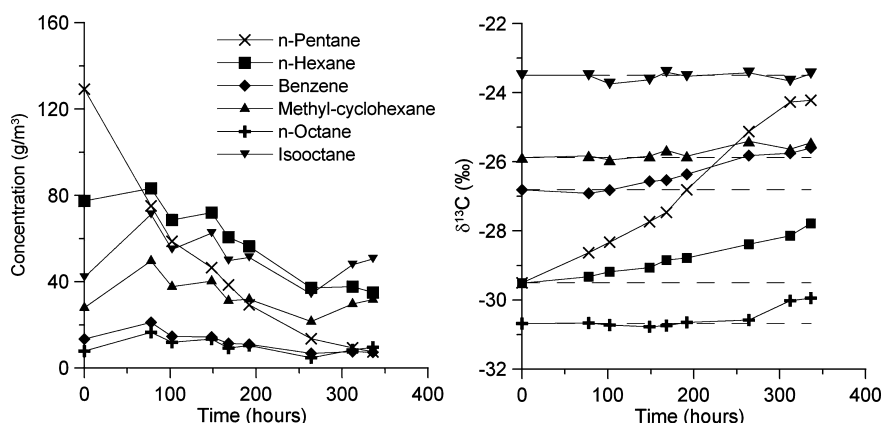


FIGURE 3. Concentration and  $\delta^{13}\text{C}$  values of gaseous samples at the source. The dashed lines illustrate the  $\delta^{13}\text{C}$  of the pure compounds used in the study.

the same column setup (21). Therefore, the concentration trends will not be evaluated in detail in this study and the discussion focuses on the isotope evolution.

During the initial 26 h of the experiment, the compounds became depleted in  $^{13}\text{C}$  by up to  $-4.8\text{‰}$  with increasing distance from the source. The depletion trend is related to transient-state diffusion and can be explained by differences in diffusion coefficients between light and heavy molecules. A similar effect was observed previously in a field experiment with hydrocarbon vapors (20) and for gases such as  $\text{CO}_2$  or methane (15–17, 19). Molecules with only light isotopes diffuse faster through the column than molecules with a heavy isotope. This tendency was observed for all compounds, but to a different extent. The supplemental weight of a heavy carbon is more relevant in small molecules, and the difference in diffusion coefficients between light and heavy molecules

is thus more pronounced (Table 1). As expected, the largest negative shift ( $-4.8\text{‰}$ ) was observed for *n*-pentane (C5) and the smallest shift ( $-1.4\text{‰}$ ) for isooctane (C8). A similar trend was recently observed in a field study where shifts between  $-4.1$  and  $-5.7\text{‰}$  were observed for C6 compounds, whereas the shift was only  $-2.1\text{‰}$  for a C9 compound (20).

At  $t = 26$  h  $\delta^{13}\text{C}$  variations with distance where  $<0.75\text{‰}$  for all compounds except *n*-octane, which was likely affected by biodegradation as indicated by the large biodegradation rate. The effect of biodegradation on isotope profiles will be discussed further below. For isooctane and MCH (except at 336 h) the isotope profile remained uniform at a  $\delta^{13}\text{C}$  corresponding to that of the source. For these compounds, diffusion probably took place under steady state conditions as indicated by the relatively stable concentration profiles for  $t > 12$  h and the biodegradation rate constants were small

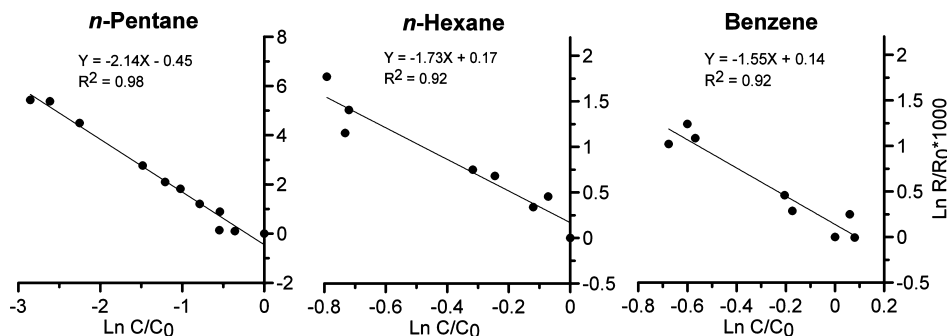


**FIGURE 4.** Relative isotope ratio ( $R/R_0$ ) as a function of the concentration decrease ( $C/C_0$ ) in the source on a natural logarithm basis during 14 days.

(Table 1). As demonstrated in S3 in the Supporting Information, under steady state conditions and in absence of biodegradation, uniform isotope profiles are expected despite of the difference in the diffusion coefficients between light and heavy molecules. The nearly uniform isotope profiles of *n*-pentane and benzene during later periods suggest that for these compounds diffusion takes place under quasi-steady state conditions as the source concentration slowly decreases.

In addition to the initial transient-state diffusion effect, a steady increase of the  $\delta^{13}\text{C}$  of compounds with a decreasing source concentration was observed for some compounds. Previous laboratory studies carried out in open vessels in fume hoods postulated a depletion in  $^{13}\text{C}$  for volatilizing sources (11, 12, 14), and therefore this process requires a more in-depth discussion. In the experiments that we present here, the source was separated from the atmosphere by a layer of sand, and gas-phase diffusion through sand controlled the rate of volatilization. Although the  $\delta^{13}\text{C}$  is expected to be constant as a function of distance under steady-state conditions (see above), the diffusive mass flux of light molecules is larger than that of heavy isotopes compared to their abundance in the source and hence light molecules are lost preferentially from the source. As demonstrated in a theoretical development in S1 in the Supporting Information, the corresponding isotope shift in the source is expected to follow a Rayleigh trend with an isotope fractionation factors corresponding to eq 2. Indeed the data for *n*-pentane, *n*-hexane, and benzene, the compounds with shifts  $>1\text{‰}$  at the source, closely follow a Rayleigh trend (Figure 4) with isotope enrichment factors of  $-2.14 \pm 0.22\text{‰}$ ,  $-1.73 \pm 0.52\text{‰}$ , and  $-1.55 \pm 0.45\text{‰}$ , respectively, determined based on eq 5 and reported with the 95% confidence interval. These measured isotope enrichment factors were compared to theoretical isotope enrichment factors calculated according to eq 2. For the considered compounds, vapor pressure differences can be neglected as indicated by differences in  $\delta^{13}\text{C}$  between pure compounds and initial source vapor  $<0.27\text{‰}$  ( $t = 5$  and  $12$  h). This is consistent with previous observations for BTEX where isotope enrichment factors of  $\leq 0.2\text{‰}$  were observed during equilibrium volatilization (11). Hence the ratio between vapor pressures in eq 2 was set to 1, whereas the ratio between the diffusion coefficients was calculated based on the molecular masses using eq 3. Theoretical isotope enrichment factors of  $-2.18\text{‰}$  for *n*-pentane,  $-1.62\text{‰}$  for *n*-hexane, and  $-1.91\text{‰}$  for benzene were obtained, which fall within the 95% confidence interval of the measured values. The good agreement confirms that the source isotope evolution is dominated by a diffusion isotope effect as previously postulated based on the results of a field study where also a  $^{13}\text{C}$  enrichment at the source was observed (20). At the field site, the enrichment in  $^{13}\text{C}$  (up to  $9.5\text{‰}$ ) was stronger than in this laboratory study, likely because the total mass loss at the field site was larger than in this column study. While in this study and in a recent field study a depletion of  $^{13}\text{C}$  is observed at the source, previous

laboratory experiments on volatilization only of organic liquids reported the inverse trend, i.e., a depletion of  $^{13}\text{C}$  corresponding to an inverse isotope effect. The different behavior in the different studies can be explained using eq 2. During volatilization, the diffusion term equals 1 and the small vapor pressure isotope effect becomes apparent if precise measurements are made. It is important to note that the diffusion effect is not expected to dominate for all compounds and elements over the vapor pressure effect during volatilization and diffusion across a porous medium. For example, for hydrogen isotopes in petroleum hydrocarbons, the diffusion isotope effect will remain the same (addition of 1 mass unit), whereas a significant inverse isotope effect can be observed during volatilization (25). The latter is expected to dominate and hence a shift of the  $\delta^2\text{H}$  in the opposite direction compared to carbon should occur.

During biodegradation of organic compounds under water-saturated conditions, typically an enrichment of  $^{13}\text{C}$  in flow direction is observed in column and field studies. In this study, only small changes in  $\delta^{13}\text{C}$  were observed along the column at  $t > 26$  h. For example, at  $t = 145$  h, the changes in  $\delta^{13}\text{C}$  were  $<0.92\text{‰}$  for all compounds including *n*-octane despite its substantial degradation rate constant. At other time periods slightly larger shifts were observed for *n*-octane, *n*-hexane, and MCH which, however, generally remained below  $2\text{‰}$ . To evaluate if such small changes are consistent with the occurrence of biodegradation, the expected shift in  $\delta^{13}\text{C}$  at steady state was calculated using the estimated biodegradation rate constants (Table 1) and isotope enrichment factors (26) determined in a separate batch study (see S4 in the Supporting Information for calculation procedure). The calculated shifts were smaller than  $0.46\text{‰}$  and deviated less than  $0.32\text{‰}$  from the measured shifts confirming that biodegradation has only a small effect on the isotope profiles. In a diffusion-controlled system, it is not possible to use a classical Rayleigh plot for further evaluation of the effect of biodegradation because the concentrations decrease along the column even in absence of biodegradation unlike in an advection-controlled column. However, instead of the concentration, the mass-flux can be related to the  $\delta^{13}\text{C}$  and an effective isotope enrichment factor can be estimated (see S4 in the Supporting Information). Such a plot based on calculated data reveals that the obtained effective isotope enrichment factor ( $-0.14\text{‰}$ ) is much smaller than the actual isotope enrichment factor ( $-1.1\text{‰}$ ) on which the calculation was based (Supporting Information Figure S2). In other words, for a diffusion-controlled system, the shift in  $\delta^{13}\text{C}$  per unit of decrease of mass flux is smaller than in an advection-controlled system, which explains why relatively small shifts in  $\delta^{13}\text{C}$  occurred despite substantial degradation for some compounds (e.g., *n*-octane). A similar observation was previously also made for diffusion and biodegradation of methane (18). In a diffusion-controlled system, the preferential removal of molecules with  $^{12}\text{C}$  during biodegradation enhances their concentration gradient and hence the cor-

responding enrichment of the heavy isotope is partly lost again due to an enhanced mass flux of light molecules.

**Field Implication.** For contaminations in the unsaturated zones, isotope monitoring may become a useful tool to identify a strong mass loss of compounds in the source based on the enrichment of  $^{13}\text{C}$  during source volatilization as observed in this study and a previous field experiment (20). The mathematical expression developed in this study potentially makes it possible to quantify the amount of removal of a compound in the source. Another potential application of isotopes in unsaturated zone studies is to link VOCs found at the surface (e.g., in a building) to a subsurface NAPL source and to distinguish them from other sources (e.g., atmosphere). This study indicates that as long as biodegradation is only moderate or fractionates little and compound loss from the source is small, the isotope signature of the source is transmitted outward due to the expected uniform isotope profiles. Such a conservative trend was, for example, observed for *n*-octane in a field experiment where  $\delta^{13}\text{C}$  values varied less than 1‰ from the source value over a distance of up to 3 m (20). Hence, for such compounds, the isotopic composition of the subsurface source can potentially be characterized based on gaseous samples even if the samples are taken at some distance from the source. Finally, if isotopes are to be used to demonstrate biodegradation of organic compounds, it has to be considered that effective isotope enrichment factors are smaller than for an advection-controlled system, and hence, it can be more challenging to detect shifts associated with biodegradation. Hence, it may be useful to measure hydrogen isotopes in addition to carbon isotopes, which tend to show a larger enrichment during biodegradation.

### Acknowledgments

We acknowledge financial support provided by the Swiss Federal Office for Education and Research in the frame of COST Action 629.

### Supporting Information Available

S1, Quantification of isotope fractionation during volatilization and diffusion across a porous medium. S2, Quantification of biodegradation. S3, Isotope evolution under steady state conditions in absence of biodegradation. S4, Quantification of isotope fractionation during biodegradation. This material is available free of charge via the Internet at <http://pubs.acs.org>.

### Literature Cited

- Mercer, J. W.; Cohen, R. M. A review of immiscible fluids in the subsurface: properties, models, characterization, and remediation. *J. Contam. Hydrol.* **1990**, *6*, 107–126.
- Baehr, A. L.; Stackelberg, P. E.; Baker, R. J. Evaluation of the atmosphere as a source of volatile organic compounds in shallow groundwater. *Water Resour. Res.* **1999**, *35*, 127–136.
- Falta, R. W.; Javandel, I.; Pruess, K.; Witherspoon, P. A. Density-driven flow of gas in the unsaturated zone due to the evaporation of volatile organic compounds. *Water Resour. Res.* **1989**, *25*, 2159–2169.
- Elsner, M.; Zwank, L.; Hunkeler, D.; Schwarzenbach, R. A new concept linking observable stable isotope fractionation to transformation pathways of organic pollutants. *Environ. Sci. Technol.* **2005**, *39*, 6896–6916.
- Hunkeler, D.; Chollet, N.; Pittet, X.; Aravena, R.; Cherry, J. A.; Parker, B. L. Effect on source variability and transport processes on carbon isotope ratios of TCE and PCE in two sandy aquifers. *J. Cont. Hydrol.* **2004**, *74*, 265–282.
- Baertschi, P.; Kuhn, W.; Kuhn, H. Fractionation of isotopes by distillation of some organic substances. *Nature* **1953**, *171*, 1018–1020.
- Jancso, G.; Van Hook, W. A. Condensed phase isotope effects (especially vapor pressure isotope effects). *Chem. Rev.* **1974**, *74*, 689–750.
- Bartell, L. S. Isotope effects on molar volume and surface tension - simple theoretical model and experimental data for hydrocarbons. *J. Chem. Phys.* **1966**, *44*, 457.
- Slater, G. F.; Dempster, H. S.; Lollar, B. S.; Ahad, J. Headspace analysis: A new application for isotopic characterization of dissolved organic contaminants. *Environ. Sci. Technol.* **1999**, *33*, 190–194.
- Balabane, M.; Letolle, R. Inverse overall isotope fractionation effect through distillation of some aromatic-molecules (anethole, benzene and toluene). *Chem. Geol.* **1985**, *52*, 391–396.
- Harrington, R. R.; Poulson, S. R.; Drever, J. I.; Colberg, P. J. S.; Kelly, E. F. Carbon isotope systematics of monoaromatic hydrocarbons: vaporization and adsorption experiments. *Org. Geochem.* **1999**, *30*, 765–775.
- Poulson, S. R.; Drever, J. I. Stable isotope (C, Cl, and H) fractionation during vaporization of trichloroethylene. *Environ. Sci. Technol.* **1999**, *33*, 3689–3694.
- Hunkeler, D.; Aravena, R. Determination of compound-specific carbon isotope ratios of chlorinated methanes, ethanes, and ethenes in aqueous samples. *Environ. Sci. Technol.* **2000**, *34*, 2839–2844.
- Huang, L.; Sturchio, N. C.; Abrajano, T.; Heraty, L. J.; Holt, B. D. Carbon and chlorine isotope fractionation of chlorinated aliphatic hydrocarbons by evaporation. *Org. Geochem.* **1999**, *30*, 777–785.
- Galimov, E. M. A  $^{13}\text{C}$  isotope enrichment effect in methane carbon in the course of its infiltration through rocks. *Geochem. Int.* **1967**, *4*, 1180–1181.
- Stahl, W.; Faber, E.; Carey, B. D.; Kirksey, D. L. Near-surface evidence of migration of natural gas from deep reservoirs and source rocks. *Bull. Am. Assoc. Pet. Geol.* **1981**, *65*, 1543–1550.
- Prinzhofer, A.; Pernaton, E. Isotopically light methane in natural gas: bacterial imprint of diffusive fractionation? *Chem. Geol.* **1997**, *142*, 193–200.
- De Visscher, A.; De Pourca, I.; Chanton, J. Isotope fractionation effects by diffusion and methane oxidation in landfill cover soils. *J. Geophys. Res.* **2004**, *109*.
- Cerling, T. E.; Solomon, D. K.; Quade, J.; Bowman, J. R. On the isotopic composition of carbon in soil carbon dioxide. *Geochim. Cosmochim. Acta* **1991**, *55*, 3403–3405.
- Bouchard, D.; Hunkeler, D.; Gaganis, P.; Aravena, R.; Höhener, P.; Kjeldsen, P. Carbon isotope fractionation during migration of petroleum hydrocarbon vapors in the unsaturated zone: field experiment at Værløse Airbase, Denmark, and modeling. *Environ. Sci. Technol.* **2008**, *42*, 596–601.
- Höhener, P.; Duwig, C.; Pasteris, G.; Kaufmann, K.; Dakhel, N.; Harms, H. Biodegradation of petroleum hydrocarbon vapors: laboratory studies on rates and kinetics in unsaturated alluvial sand. *J. Contam. Hydrol.* **2003**, *66*, 93–115.
- Coplen, T. B. New guideline for reporting stable hydrogen, carbon, and oxygen isotope-ratio data. *Geochim. Cosmochim. Acta* **1996**, *60*, 3359–3360.
- Craig, H. The geochemistry of stable carbon isotopes. *Geochim. Cosmochim. Acta* **1953**, *3*, 53–92.
- Clark, I.; Fritz, P. *Environmental Isotopes in Hydrogeology*; CRC Press: Boca Raton, FL, 1997.
- Wang, Y.; Huang, Y. Hydrogen isotopic fractionation of petroleum hydrocarbons during vaporization: implication for assessing artificial and natural remediation of petroleum contamination. *Appl. Geochem.* **2003**, *18*, 1641–1651.
- Bouchard, D.; Hunkeler, D.; Höhener, P. Carbon isotope fractionation during aerobic biodegradation of *n*-alkanes and aromatic compounds in unsaturated sand. *Org. Geochem.* **2008**, *39*, 23–33.
- Lugg, G. A. Diffusion coefficients of some organic and other vapors in air. *Anal. Chem.* **1968**, *40*, 1072–1077.